Environmental Science

Volume 2, Issue 3, 547-564.
DOI: 10.3934/environsci.2015.3.547
Received date 7 April 2015,
Accepted date 10 June 2015,
Published date 11 June 2015

http://www.aimspress.com/

Research article

Study of a complex environmental mixture by electrospray ionization and laser desorption ionization high resolution mass spectrometry: the cigarette smoke aerosol

Vincent Carré [1,*], Sébastien Schramm [2] and Frédéric Aubriet [1]

[1] Laboratoire de Chimie et de Physique – Approche Multi-échelles des Milieux Complexes, Université de Lorraine. Institut Jean Barriol (FR CNRS 2843) / TGE FT-ICR (FR CNRS 3624), 1, Boulevard Arago, F-57070 Metz Technopole Cedex 03, France
[2] CEA, DAM, DIF, F-91297 Arpajon, France

* **Correspondence:** Email: vincent.carre@univ-lorraine.fr; Tel: +33-3-87-31-5853; Fax: +33-3-87-31-5851.

Abstract: Aerosols from the mainstream cigarette smoke have been analyzed by electrospray ionization (ESI) coupled to Fourier transform ion cyclotron resonance mass spectrometry (FTICRMS). Measurements have been conducted in positive ion mode. The chemical composition of cigarette smoke aerosol is significant because it gives insights of one complex indoor environmental mixture. Almost 1300 chemical compositions relative to nitrogen species were successfully determined through the accurate mass measurement and the good ion production of the used technique. The most abundant class of compounds corresponds to N2 one (hydrocarbons with two nitrogen atoms). For other classes, the van Krevelen diagrams ensured to define that other nitrogen and oxygen-nitrogen compounds adopted similar behavior in terms of unsaturation and alkylation range. The detailed composition of cigarette smoke aerosol provided a typical chemical fingerprint from the biomass pyrolysis with tobacco-specific compounds. We examined also the contribution of laser desorption ionization (LDI) technique coupled to FTICRMS for the acute analysis of cigarette smoke aerosol. While a part of the chemical composition were found similar to ESI results, LDI achieved a broader range of poly-aromatic compounds and highlight new class compounds as pure hydrocarbon and oxygen-containing species. The combination of ESI and LDI with high resolution mass spectrometry clearly increased significantly the coverage of the "whole composition" of environmental aerosols such as cigarette smoke aerosol.

Keywords: cigarette smoke; aerosol; FTICR Mass Spectrometry; ESI; LDI; environmental analysis

1. Introduction

Risk assessment for environmental and human point of view is particularly a challenge for complex mixture exposures. Especially, it is expected that cocktail of chemicals is even more dangerous as a mix. But, the first barrier is linked to the chemical identification of such mixtures at the molecular level. It is more specifically the case for the condensed matter generated by the combustion of fuel, biomass or waste which is released in outdoor and indoor environments. Their chemical composition is sparsely covered because of their huge chemical diversity and the restricted number of compounds identified by the commonly used targeted analytical approach. Consequently, to address a full chemical characterization of a complex mixture, a non-targeted approach has to be considered. Such strategy pushes the analytical techniques to their limits and high performance instruments have to be used. In this context, we develop an innovative approach to investigate complex mixture composition.

This study is focused on the cigarette smoke aerosol which is a major concern among indoor air pollution. Indeed, more than 5600 compounds have been identified in cigarette smoke and unidentified compounds may be as high as 100,000 [1,2]. Cigarette smoke is constituted by both vapor and condensed phases. Whereas the gas phase species are fairly documented [3-8], the condensed fraction is up to now only poorly known [9-13]. Its chemical analysis systematically requires pretreatment, purification, concentration and separation steps by chromatography setups to yield data on a restricted number of targeted compounds. For example, tobacco-specific nitrosamines (TSNA) were identified and quantified with nicotine in mainstream cigarette smoke by LC-MS/MS after particulate matter extraction [14]. Benzo(a)pyrene as well as 10 other PAHs were selectively extracted, purified and quantified in mainstream cigarette smoke by GC-MS [15].

To perform untargeted analysis of such complex sample, one analytical approach consists in integrating different and orthogonal separation systems to increase the separation capability. Thus, the comprehensive GC×GC-TOFMS demonstrated a good ability to describe a lot of cigarette smoke aerosol components [16,17,18]. Another way is to use the high resolution mass spectrometry, which demonstrated a very high capability to identify with high sensitivity and mass measurement accuracy an impressive number of compounds in complex mixtures without chromatographic separation steps [19,20,21]. Moreover, the coupling of direct-infusion electrospray ionization (DI-ESI) with high resolution mass spectrometry is able to chemically resolved complex environmental mixtures [22] as organic fraction of atmospheric aerosol or dissolved organic matter [23-27]. To increase the number of identified chemicals in cigarette smoke aerosols, the use of high resolution mass spectrometry with ESI may be considered as a valuable alternative technique. Consequently, we performed, for the first time, the analysis of cigarette smoke aerosol by direct infusion ESI Fourier transform ion cyclotron resonance mass spectrometry (DI-ESI-FTICRMS). For this purpose, mainstream cigarette smoke was bubbled into successive liquid impingers which ensured the simultaneous collection of a portion of the volatile compounds and the particulate phase. In a previous work, we specifically collected a large part of particulate matter from cigarette smoke on quartz-fiber filters. Subsequent high resolution mass spectrometry analyses were performed by laser desorption/ionization (LDI) of such loaded filters. As this technique succeeded to provide a sufficient comprehensive chemical

composition to discriminate different cigarette smokes [28,29], LDI-FTICRMS was also used to investigate the cigarette smoke aerosol collected in a solvent.

2. Materials and Method

2.1. Sample collection

The cigarettes used in this study were commercially available European cigarettes, which deliver 0.60 mg of nicotine, 8 mg of carbon monoxide and 7 mg of tar according to the manufacturer. Cigarettes have been smoked using a home-building smoking machine. According to the ISO/FTC smoking procedure, each cigarette was smoked at one puff per minute, 2 s puff duration, and 35 mL puff volume. The mainstream cigarette smoke was bubbled into three successive 100-mL gas washing bottles, which contained 50 mL of acetonitrile. At the end of the experiment, the three acetonitrile solutions were pooled, adjusted at a final volume of 250 mL (the so-called acetonitrile extract) and, stored in the dark at 4 °C before the analysis by high resolution mass spectrometry, without other additional preparation (no filtration neither addition of chemicals as TFA). Acetonitrile was chosen due to its significant capability to generate a stable electrospray and its ability to dissolve a large range of compounds.

This mainstream cigarette smoke collection methodology ensures to obtain a "whole acetonitrile extract" that gathered the volatile compounds which are readily soluble in acetonitrile and the organic compounds which constitute the aerosol and/or are adsorbed at its surface.

2.2. High resolution mass spectrometry

High resolution mass measurements were conducted in the positive ion detection mode on an IonSpec HiRes Fourier transform ion cyclotron resonance mass spectrometer (Varian-IonSpec Corporation, Palo Alto, CA, USA) fitted with an actively shielded 9.4-tesla superconducting magnet (Cryomagnetics, Oak Ridge, TN). Negative ion mass spectra were also acquired but it was chosen to only present in this publication the positive ion results. Indeed, the trends observed with the different investigated samples were compared and were found to be similar whatever the used ion polarity (positive or negative). Before acquisition, the mass spectrometer is externally calibrated by considering the cluster ions produced by the LDI of graphite for LDI-FTICRMS or a standard calibration mixture for ESI-FTICRMS. After the acquisition, the obtained mass spectrum was internally recalibrated according to some peaks which were unambiguously identified. The elemental composition of each detected signal with a signal-to-noise ratio (S/N) greater than 3 was determined by using Omega 8 Elemental Composition software (Varian-IonSpec Inc) with the following search criteria: $C_{6–100}{}^{13}C_{0–2}H_{6–100}N_{0–20}O_{0–20}S_{0–5}K_{0–5}$ general formula and a 2 ppm tolerance error. The addition of other atoms such as sodium did not modify the obtained assignments. When it was possible, the isotopic pattern was checked with Omega 8 Exact Mass Calculator software (Varian-IonSpec Inc).

2.2.1. Electrospray ionization

ESI experiments were performed with a Micromass Z-spray external ESI source. Freshly

prepared sample was directly and continuously infused in the source region at a flow rate of 2 $\mu L \cdot min^{-1}$. The used high voltage (HV) ranged from −3800 to −4200 V. Nitrogen was used as drying gas. The temperature of the source and the probe were kept to 80 and 100 °C, respectively. The sample cone voltage was fixed at 45 V and the extraction cone was kept constant to 10 V. Extracted ions were accumulated in a RF-only hexapole for 2 s before to be transferred to the ICR cell.

2.2.2. Laser desorption ionization

For LDI experiments, the external ion source ProMaldi card was used. Cigarette smoke aerosol sample (2 µL of the final solution) was deposited on a stainless steel sample holder prior to introduction into the source of the mass spectrometer. Ions were generated by LDI of the sample with an ORION air-cooled Nd:YAG laser system (New Wave Research Inc, Fremont, CA) working at the 355 nm wavelength (laser pulse duration 5 ns). The laser power was fixed to 0.9 $J \cdot cm^{-2}$, which allows fragmentation processes to be avoided and intense signals to be obtained. The ions resulting from eight successive laser-sample interactions were stored in a RF-only hexapole before to be transferred to the FTICR cell. There were 200 ms between the different laser pulses. After each laser pulse, the sample stage was moved such that ions were generated from a fresh (not previously ablated) target area. Stage motion is on the order of 100–200 µm. To thermalize ions during their accumulation in the storage hexapole, N_2 was introduced by a pulsed valve.

2.2.3. Ion transfer and FTICR mass measurement

To guide ions to the ICR cell, a second hexapole was tuned to optimize transfer of ions in the 120–500 m/z range. After their transfer, ions were trapped in the ICR cell with a 0.2 V trapping potential where the residual pressure was around 10^{-10} mbar. M/z 100 to 1500 ions were then excited by the application of an arbitrary excitation wave function on the excitation plates. The resulting image current was detected, amplified, digitized, apodized (Blackman) and Fourier-transformed to produce a mass spectrum. It has to be noted that LDI-FTICRMS system ensured to detect lower mass compounds than ESI. This was not due to a lower sensitivity of ESI-FTICRMS to such compounds but it was relative to a technical constraint. The RF of the transfer hexapole is greater for the LDI-FTICRMS system than for the ESI-FTICRMS one, which induces a more effective transfer of low m/z ions from LDI ion source.

Typically, the average mass measurement accuracy is better than 500 ppb, and the mass resolution is between 500,000 and 2,000,000 at 150 m/z. Re-processing of the mass spectrum of cigarette smoke aerosol was performed by re-calibration of the most intense mass peaks (N2 class).

3. Results and Discussion

3.1. High resolution mass analysis of cigarette smoke aerosol by ESI-FTICRMS

The direct infusion (DI) of the cigarette smoke sample leads to a very complex ESI mass spectrum. The positive ion signals are distributed in the 150 to 400 m/z range. The very high mass resolution achieves in this study (between 500,000 and 2,000,000 in the 150 to 400 m/z range) allows us to distinguish more than 1300 peaks on the mass spectrum reported in the Figure 1. As an

example, seven peaks are observed in a 0.16 m/z range around the 197 nominal mass and, a chemical formulae was successfully assigned to each of them (Figure 1). The average mass accuracy measurement is better than 450 ppb, which ensures to assign an unambiguously elemental composition to 1275 mass peaks (the figure of merit for the ion mass measurement accuracy is given in supplementary material).

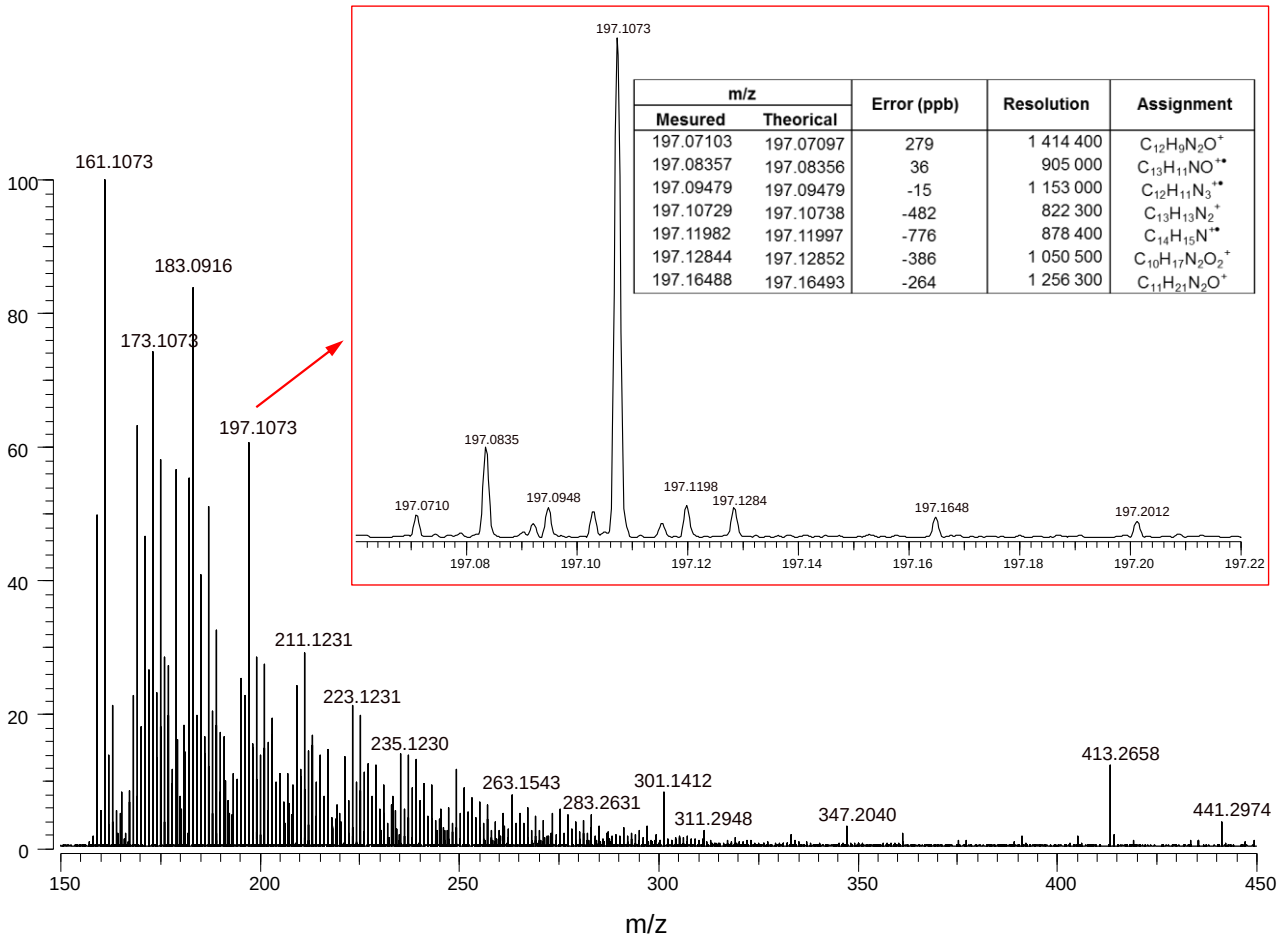

Figure 1. ESI-FTICR mass spectrum of cigarette smoke aerosol in positive ion mode. 1275 peaks were identified. In caption, the magnification of a 0.16 Da range around m/z 197 and the assignment of detected ions.

Except some peaks, which are associated with phthalate contaminants (the dioctyl phthalate $C_{24}H_{38}O_4$ at m/z 301.1412 $[M - C_8H_{16} + Na]^+$ and 413.2658 $[M + Na]^+$ and, the dinonyl phthalate at m/z 441.2974 $[M + Na]^+$), the main part of the detected organic compounds are relative to $C_nH_mN_z$ species. Most of them are detected as protonated ions and to a lesser extent as radical cations. Note that radical species only represent less than 15 % of the total ion current (TIC). Rather than to be the result of the fragmentation of larger protonated ions, these radical cations are thought to be generated by electrochemical oxidation phenomenon as it was previously reported especially in positive-ion [30]. The observation a radical cation is always associated with the detection of the corresponding protonated and/or deprotonated cation, which relative abundance generally ranges between 25 to 100%.

More specifically, the $C_nH_mN_2$ compounds are the most abundant species detected as reported in

Figure 2. Indeed, this N2 class includes alkaloids as nicotine ($C_{10}H_{14}N_2$) which is known to be transferred in large amounts to the mainstream cigarette smoke without alteration [5].

The third of the TIC is also associated to nitrogen-containing compounds with at least one oxygen atom. Among them, some ions have to be assigned to known compounds as specific to tobacco smoke. For example, $C_{10}H_{12}N_2O$ compounds (cotinine and/or isomers), $C_9H_{11}N_3O$ and $C_{10}H_{13}N_3O_2$ species which were tentatively assigned to nitrosamines (NNN and NNK) are observed.

The relative distribution of nitrogen-containing species looks like very similar to what it was observed in the ESI positive ion study of bio-oils generated by pyrolysis of different feedstock [31,32]. This suggests that the pyrolysis products of the different tobacco leaf components (proteins, lipids, sugar, cellulose, hemicellulose, lignin, …) contribute to the cigarette smoke [33]. As an example, the imidazole $C_3H_4N_2$ heteroaromatic functional group is associated to pyrolysis products of histidine. Consequently, the pyrolysis of tobacco leaf proteins contributes to N2 class of compounds [31].

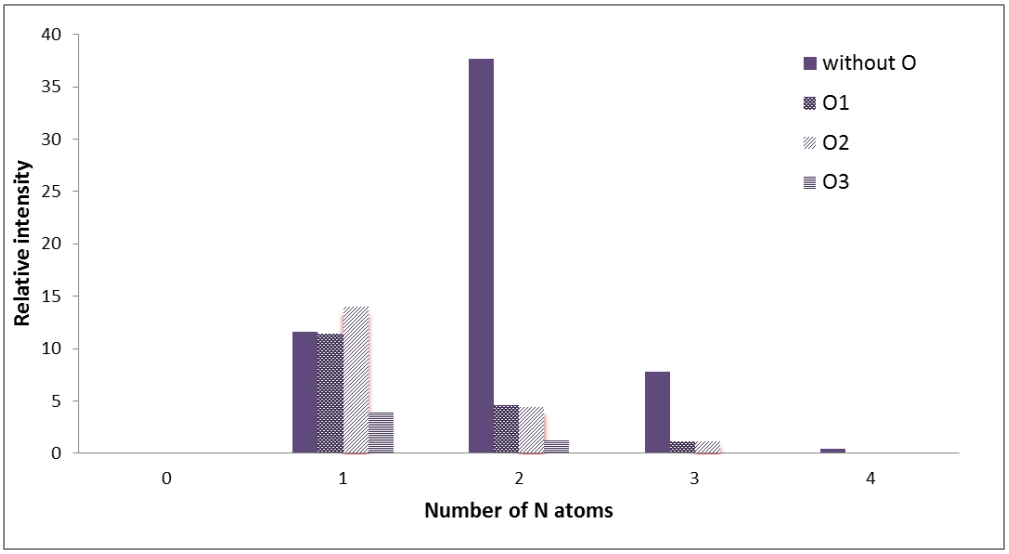

Figure 2. Relative distribution of $C_nH_mN_zO_p$ classes observed by ESI-FTICRMS for chemical compounds containing a various number of oxygen (0 to 3) and nitrogen (0 to 4) atoms.

The huge number of signals generally detected by a non-targeted analytical approach complicates the analysis of the results. Indeed, the main difficulty of high-resolution mass spectrum of a very complex organic sample is to clearly and simply visualize a large amount of information. In this way, different graphical representations have been used: 2-D Kendrick maps as well as 3-D Van Kreleven diagrams [34, 35].

A 2-D Kendrick map reports for a given data set, the Kendrick mass defect (KMD) in respect with the nominal mass for each mass peak (see the Supplementary Material for KMD calculation). The Kendrick map for the data reported in Figure 1 was given in Figure 3a.

Three periodicities appear on the 2-D Kendrick maps of the investigated cigarette smoke sample. The first one (① indexed) gathered compounds which only differ by one or several methylene (CH_2) groups. Consequently, these signals correspond to the same class of compounds but to different hydrocarbon skeleton and to an increment from left to right of a methylene group on a given

structure, which modifies the nominal mass by 14 but not the KMD. The ② indexed periodicity gathers species, which only differ by the number of unsaturations. Additional unsaturation induces a two nominal mass decrease and an increase of KMD by 0.0134. An increase of half of this KMD increment and the decrease of the nominal mass by one mass unit corresponds the $[M + H]^+$ and $M^{+\bullet}$ ions of the same compound, respectively. This is especially the case with high unsaturated species. Finally the third periodicity (the ③ one) corresponds to the substitution of 1, 2, 3 or 4 methylene groups, which mass is 14.01565 Da by 1, 2, 3 or 4 nitrogen (14.00307 Da) atoms. This induces a slight shift of the KMD.

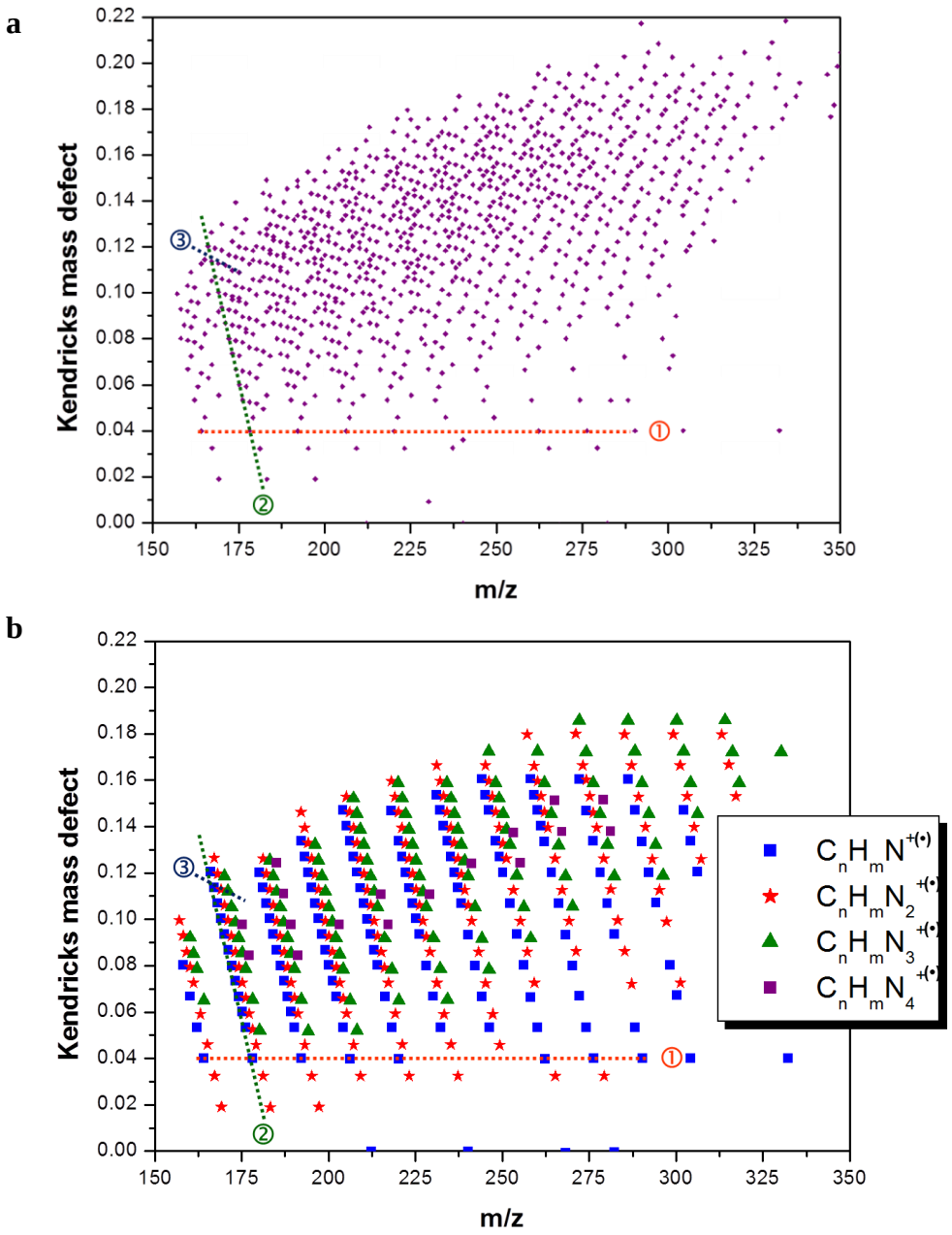

Figure 3. 2-D Kendrick maps for (a) the data set presented on the Figure 1 and for (b) $C_nH_mN_{1-4}^+$ and $C_nH_mN_{1-4}^{+\bullet}$ ions.

To obtain an easy readable 2-D Kendrick map, a restricted number of classes of compounds has to be reported. For example, the Figure 3b specifically displays the $C_nH_mN_{1-4}^+$ and $C_nH_mN_{1-4}^{+\bullet}$ ions. It can be observed that numerous nitrogen-containing compounds are distributed on a broad range of unsaturation. For each unsaturation value, the saturated part of those molecules which reflects the degree of alkylation can range up to 12 carbon atoms. This data description has to be seen as a complementary view point of the relative distribution of $C_nH_mN_z$ reported in the Figure 2. Similar analysis and data treatment have been done with N and N_3 classes of compounds. The obtained 2-D Kendrick maps look like very similar, which means that their average degree of unsaturation and alkylation (extension of the hydrocarbon skeleton) are globally identical for all nitrogen-containing compounds present in the cigarette smoke whatever the number of nitrogen atoms. Moreover, the high dynamic range of the analysis reveals very accurate details on molecular composition of each class of compounds.

The Figure 2 clearly evidences the concomitant presence of oxygen and nitrogen atoms for a large amount of cigarette smoke components. To clearly represent on a same graph the elemental composition of these compounds, the three-dimension van Kreleven diagram is used. For each obtained molecular formula, the H/C, O/C and N/C atomic ratios are calculated and correspond to the *x*, *y* and *z* cartesian coordinates of the dot associated to this signal. In respect with the number of unsaturation, oxygen and nitrogen atoms, different lines and clouds are visible in the 3-D van Krevelen diagram (Figure 4). In spite of the usefulness of this data representation, it has to be noted that the information of the *m/z* ratio is lost and additional 2-D Kendrick maps are required to fully represent and account of the detected species.

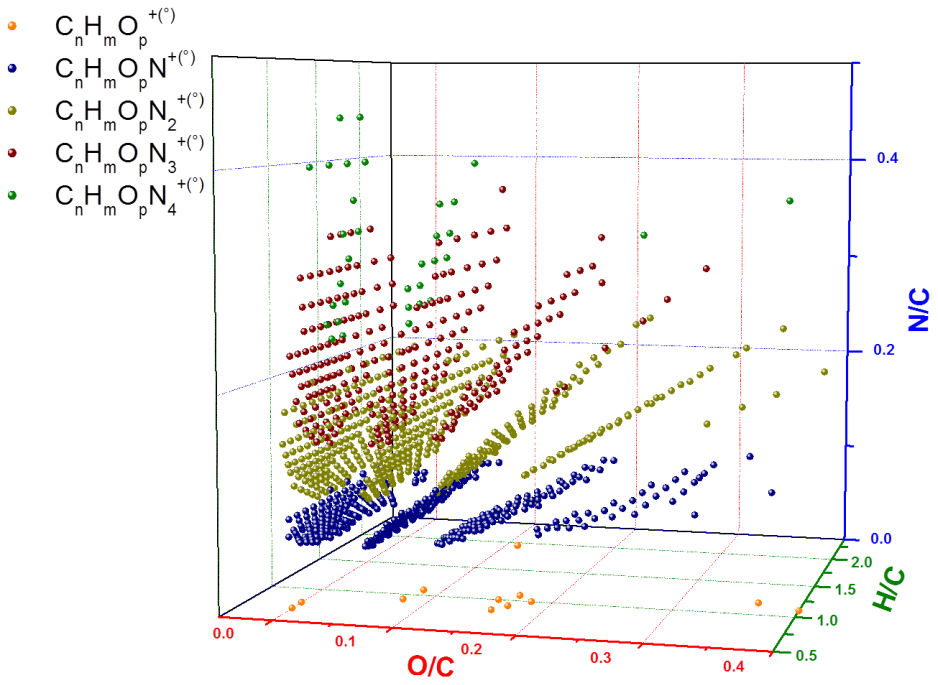

Figure 4. 3-D van Krevelen diagram of species detected by ESI-FTICRMS in a cigarette smoke aerosol.

Although oxygen species contribute weakly to the TIC of nitrogen-containing organic species on the mass spectrum, the diversity of composition evidences on the Figure 4 is important. Whatever the number of nitrogen or oxygen atoms in the detected species, the unsaturation range, which is directly connected to the H/C value, seems to be similar. An averaged value close to 1.2 is evidenced. The unsaturation degree may also be evaluated by considering the DBE values (double bound equivalent—See Supplementary Material for calculation). The DBE ranges from 2 to 14 with a quasi-Gaussian distribution. The highest signal intensity is generally observed for a DBE value close to 7 or 8. For the $C_nH_mN_{1-4}O_p$ species, the O/C ratio ranges from 0 to 0.3 which is relatively low in regard to the classical pyrolytic biomass region on a van Krevelen diagram. This clearly evidences that the pyrolysis of highly oxygenated components of cigarette paper and tobacco poorly contributes to the composition of cigarette smoke. The N/C dimension gives an extended view of the data. Indeed, an increase of the nitrogen content is associated to a narrowing of the unsaturation range without modification of the average DBE value.

3.2. Comparison of the electrospray and laser desorption ionization for the investigation of cigarette smoke aerosol

The electrospray ion source is highly sensitive to polar compounds but inefficient to ionize apolar molecules in mixtures. To achieve a "whole composition" of cigarette smoke aerosol, we also performed FTICRMS analysis of the same cigarette smoke sample with laser desorption ionization source (LDI).

The detected signals range from m/z 120 to 330. The assignment of the observed peaks reveals the detection of ~ 700 ions corresponding to protonated or radical ions, which obey to the $C_nH_mN_zO_p$ general formula. The radical cations are more abundant in LDI-FTICRMS, they are mainly formed by multiphoton photoionization phenomenon—i.e. interaction in the gas phase between two or three photons from the laser and neutral molecules desorbed upon laser-matter interaction. While LDI is referred to be a less soft ionization technique than ESI, the fine adjustment of the laser power density at the 355 nm wavelength and, the ion-thermalization process have to be finely adjusted to avoid or at least reduce the fragmentation phenomena.

The relative distribution of the observed signal in respect with the considered classes of compounds and, the used ionization technique is given in the Figure 5. It has to be kept in mind, that the relative intensity of ions detected by mass spectrometry is not only dependent to the relative abundances of the associated compounds in the sample. Indeed, other factors such as the ionization efficiency of a given class of compounds compared to another one and the stability of the formed ion in the gas phase may sometimes significantly affect the relative distribution of the detected ions. Consequently, the comparison of results obtained by LDI and ESI of the same sample has to include this fact.

As it is observed when the analysis of cigarette smoke aerosol is conducted by ESI, the N1 to N3 classes dominate the LDI-FTICR mass spectrum. The N2 compounds are still the most abundant species, nevertheless, the amounts of nitrogen and oxygen atoms in the detected compounds is lower for LDI than for ESI. The 3-D van Krevelen diagram confirms this fact and evidences ion clouds, which are restricted to low N/C and O/C values (Figure 6). It also appears that the unsaturation range of these species is narrower for LDI than for ESI data.

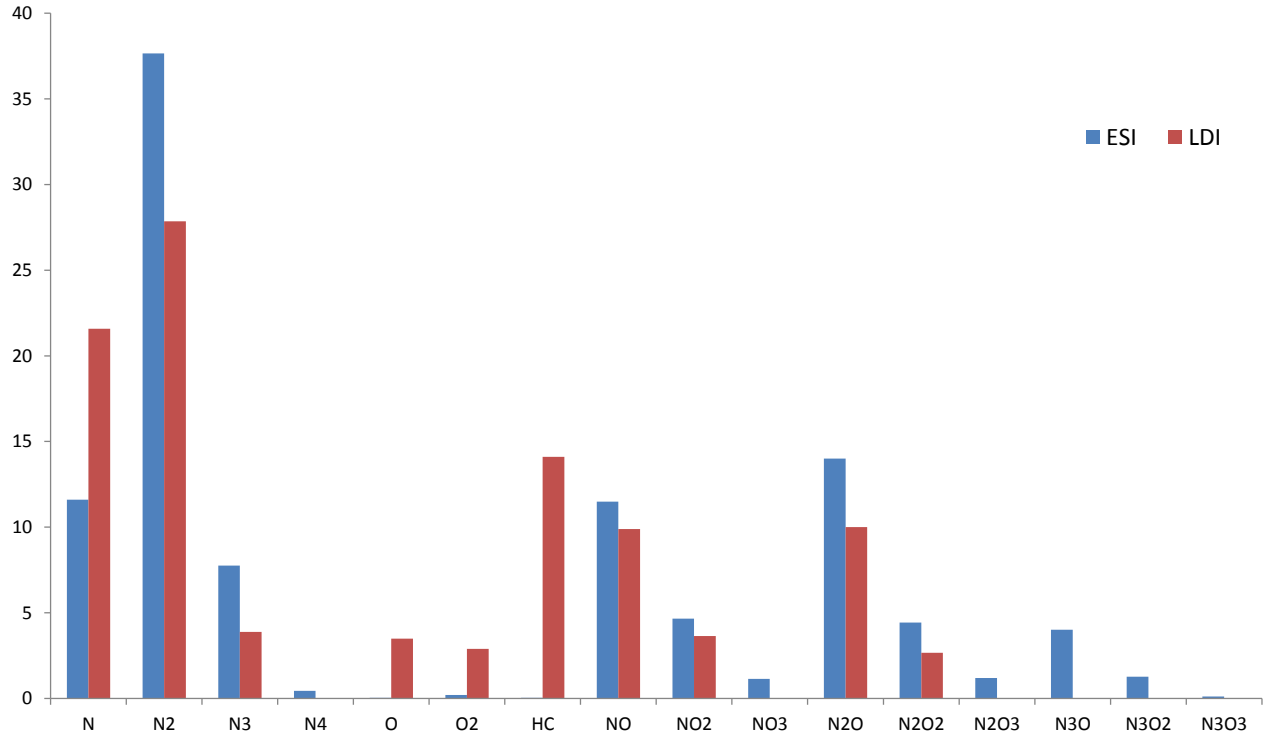

Figure 5. Relative distribution of the observed classes of compounds detected by LDI-FTICRMS (red) and ESI-FTICRMS (blue) in the analysis of a cigarette smoke sample.

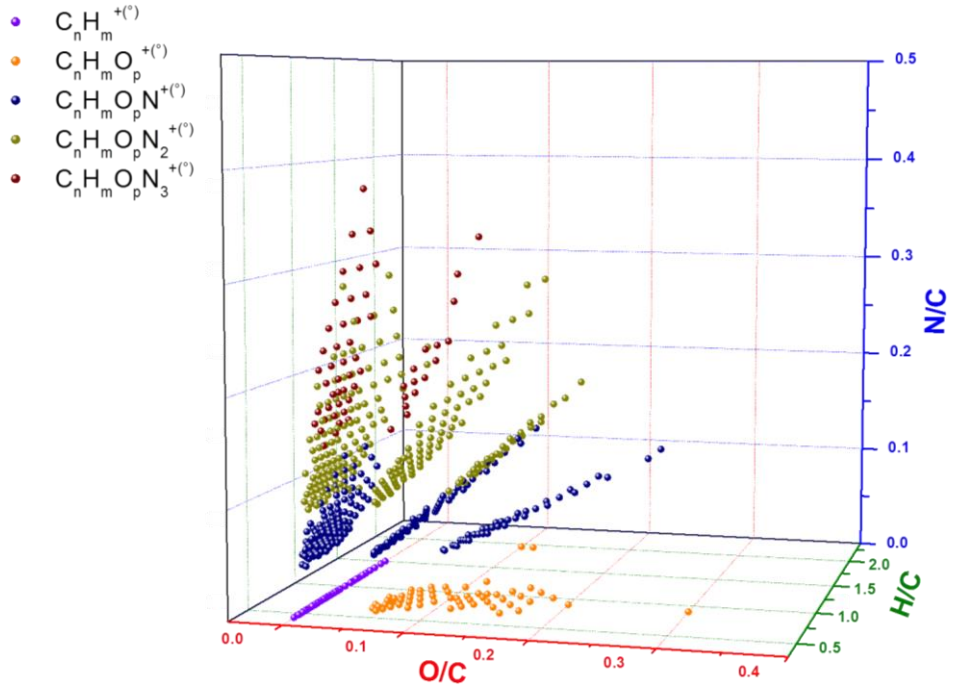

Figure 6. 3-D van Krevelen diagram of species detected by LDI-FTICRMS of a cigarette smoke sample.

Moreover, some chemical classes are found to be specifically highlighted by LDI. The first one is the pure hydrocarbons (HC class) and the second ones the oxygen-containing hydrocarbons (O1 and O2 classes). These latter are thought to content at least one aromatic ring according to the value of the DBE. The main part of them are relative to tobacco pyrolysis products whose structure is derived from guaiacol, catechol or furanylethanone [33,36,37,38]. The high DBE value of HC compounds, which is systematically higher than 8 clearly associates the presence of compounds polyaromatic hydrocarbons (See the DBE vs. C# for HC class in Supplementary Material). Polyaromatic hydrocarbons (PAHs) such as pyrene and benzopyrene, for example are detected as molecular radical ions while alkyl-PAHs are observed as non-radical species. Indeed, alkylated-PAH frequently undergo β C-C bound dissociation to yield pseudo-tropylium cation. Some of the detected PAHs and alkyl-PAHs have been reported in previous analyses of cigarette smoke [15,39,40] as well as in combustion or pyrolysis product of carbonaceous material.

To complete the comparison of ESI and LDI results, the relative distribution of ions are compared according to their DBE values (Figure 7).

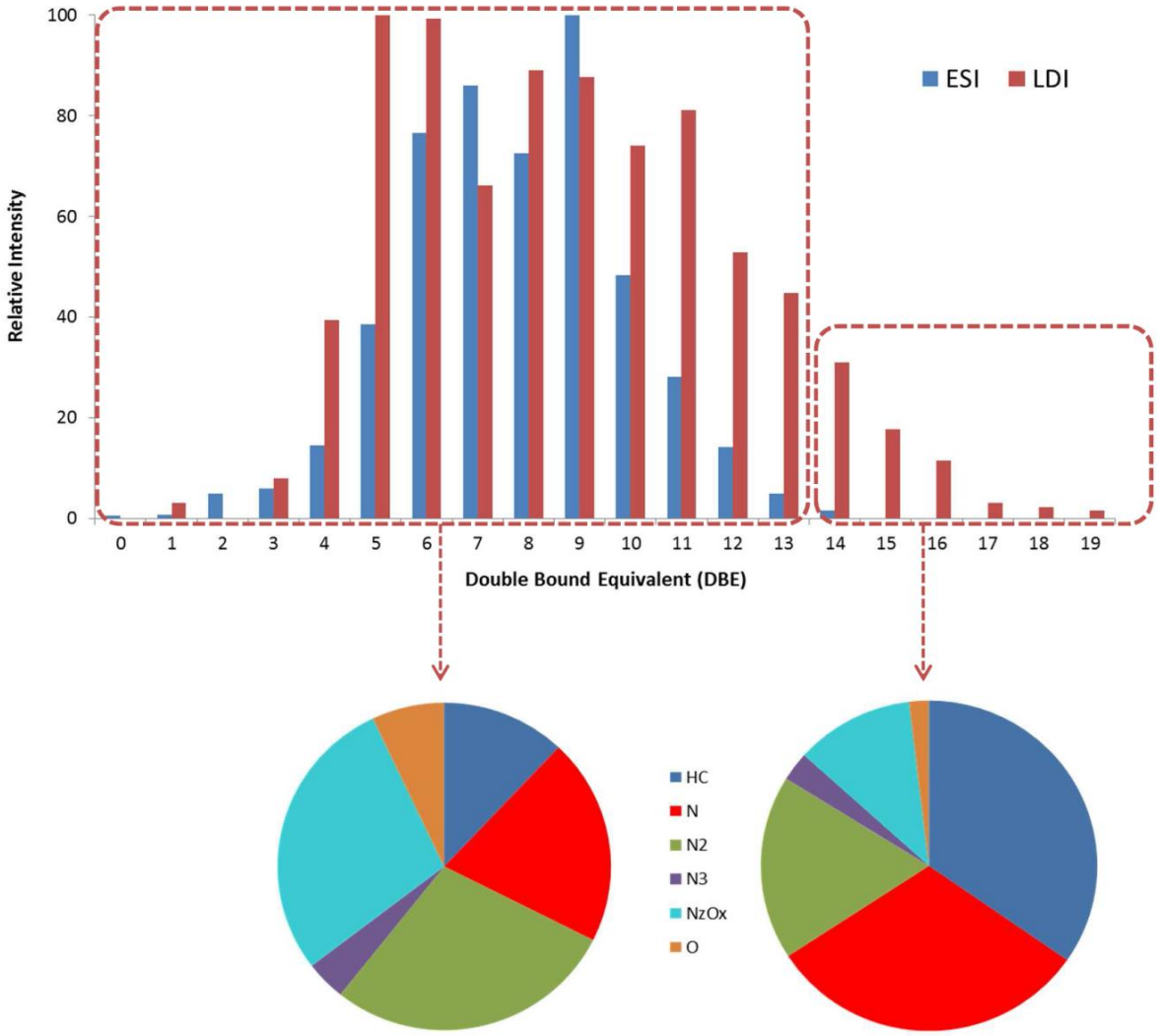

Figure 7. Relative distribution of ions detected by LDI (red) and ESI (blue)

FTICRMS depending on the DBE value—For LDI-FTICRMS, the pies reports the distribution of compound classes for the highest values of DBE (from 14 to 19) compared to the lowest ones (from 0 to 13).

Whatever the ionization technique, the main part of the detected compounds presents DBE ranging from 5 to 11. However, the range of DBE of compounds detected by LDI is broader than it is observed by ESI. Indeed, the higher DBE value observed by ESI is 14, whereas DBE extend up to 19 for compounds observed by LDI of the cigarette smoke sample.

Consequently, it is clearly evidenced, that the relative distribution of ions detected by ESI- and LDI-FTICR mass spectrometry is not solely dependent to the relative concentration of the corresponding compound in the investigated sample. The more or less efficient ionization of a given class of cigarette smoke components in respect with the used ionization technique significantly influences the nature and the distribution of the detected species. Consequently, the differences observed on the mass spectra obtained by ESI and LDI have not to be considered antagonism but relevant to the complementary ionization techniques to fully characterize the composition of a complex sample mixture. Indeed, the ESI favors the ionization of the most polar compounds of the mixture and LDI provides access to a wider range of high aromatic compounds, which are known to be non-polar compounds.

An interesting feature is observed for LDI-FTICRMS data when the class distribution is detailed for the highest unsaturated species and compared to the other ones. While every class contributes to the global intensity for compounds with a DBE value ranging from 0 to 13, the highest unsaturated species (DBE > 13) are dominated by HC and N1 classes at the expense of NOx and O compounds. Consequently, it is reasonable to consider that such species are mainly polyaromatic and heteroatomic polyaromatic compounds which are efficiently ionized by LDI [41,42,43]. This result suggests that nitrogen atom for N class compounds, is included in a pyridine ring. Consequently, these compounds are mainly azaarene as polybenzoacridine. On the contrary, according to their lower DBE values, O class involves mainly species with hydroxyl, carbonyl or ether functional group connected to an aromatic hydrocarbon skeleton which explains why O compounds with high value of DBE are weakly detected. According to the fact that NOx and O classes adopt the same behavior in respect with their relative abundance as a function of the DBE value, the oxygen atoms for NOx species are thought to be not included in hetero-aromatic ring but rather in carbonyl, hydroxyl or ether functional groups. To confirm this, NMR analyses have to be done and compared to previously published work [23,26,44]. This is still under investigation but the complementary sensitivity of ion sources in respect to the molecular structure of the compounds in a mixture is an interesting way to provide clues.

The present results on cigarette smoke aerosol may be compared to our previous investigations performed by LDI-FTICRMS after collection of cigarette smoke on quartz filters [28]. In that later case, only the condensed (particle and liquid aerosol) phase of cigarette smoke was collected and finally analyzed. For $C_nH_mN_{1-4}O_{0-3}$, the nature and the distribution of the ions which is observed, whatever the used collection method, is very similar. Nevertheless, the HC and O families are more significantly detected in this study. This is well explained by a more efficient collection process of these compounds, which are partitioned between gas and particulate matter phase. The bubbling of cigarette smoke into gas washing bottles ensures the solubilisation of organic volatile compounds as aldehyde (O1 class of compounds) or PAH (HC class of compounds). An additional explanation may

also be the influence of the substrate (stainless steel or quartz filter) on the efficiency of LDI phenomenon. Indeed, the electric or thermal conductivity as well as the reflectivity of the sample substrate may increase or decrease the ionization yield. Such phenomenon may also be "compound-dependant".

4. Conclusion

The composition of cigarette smoke aerosol obtained by ESI-FTICRMS analysis in positive ion detection mode successfully reveals more than one thousand nitrogen-containing compounds. The LDI approach confirms the identification of a large part the compounds evidenced by ESI but also provides additional information on highly unsaturated species and compounds such as polycyclic aromatic hydrocarbons, aldehydes and phenolic compounds.

Finally, it is clearly demonstrated in this paper, that the combination of ESI and LDI coupled to high resolution mass spectrometry is a powerful tool to achieve a good description of the "whole composition" of environmental contaminant such as cigarette smoke.

Acknowledgments

Financial support from the TGE FT-ICR for conducting the research is gratefully acknowledged.

Conflict of Interest

The authors declare that there are no conflicts of interest related to this study.

Supplementary

Accuracy of mass measurement of ions detected by ESI-FTICRMS of cigarette smoke

The average mass accuracy measurement is better than 450 ppb, which ensured to identify unambiguously elemental compositions to 1275 mass peaks. The figure of merit is reported in Figure S1. 50, 75 and 90 percentiles were found to be equal to 390, 690 and 960 ppb, respectively which ensure that the assignment of mass peaks to elemental composition is confident.

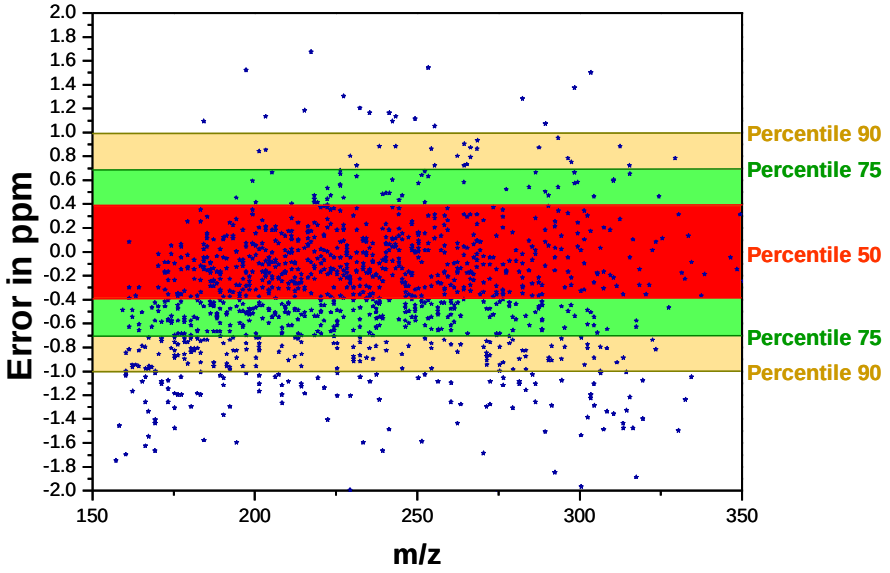

Figure S1. The figure of merit of mass measurement for ions detected by ESI-FTICRMS of cigarette smoke aerosol.

Data treatment—calculation of Kendrick mass defect (KMD) and double bound equivalent (DBE)

Kendrick map is a 2-D graphical representation of a mass spectrum and reported the Kendrick mass defect (KMD) as a function of the Kendrick nominal mass (KNM). The Kendrick mass (KM) is calculated by taking CH_2 group as mass reference instead of the mass of ^{12}C. The Kendrick mass defect (KMD) corresponds to the difference between the KM and the KNM.

$$KM = M_{measured} \times \frac{14.0000}{14.0157}$$

$$KMD = KM - KMN$$

For each elemental composition of ions, the double bond equivalent (DBE) is obtained by the following equation:

$$DBE = \frac{2n_C + 2 + n_N - n_H}{2}$$

The DBE is indicative to the number of unsaturation of each assigned ion.

Description of hydrocarbon class detected by LDI-FTICRMS

The Figure S2 corresponds to the visualization the DBE vs. C# of HC class detected by LDI FTICRMS of cigarette smoke sample. To locate the common PAHs detected, some structures are proposed.

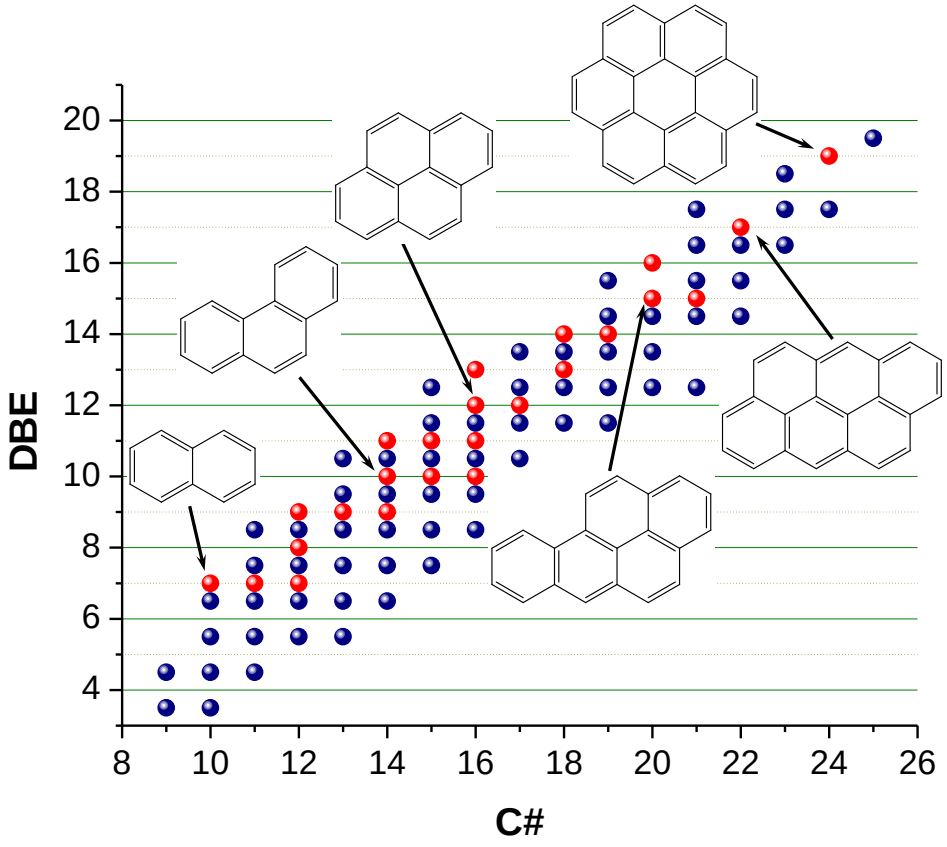

Figure S2. DBE vs. C# plot of (red) radical cations and (blue) cations for HC class compound detected by LDI-FTICRMS of cigarette smoke.

References

1. Stedman RL (1968) Chemical composition of tobacco and tobacco smoke. *Chem Rev* 68: 153-207
2. Smith CJ, Perfetti TA, Garg R, et al. (2003) IARC carcinogens reported in cigarette mainstream smoke and their calculated log P values. *Food Chem Toxicol* 41: 807-817
3. Dallüge J, van Stee LLP, Xu X, Williams J, et al. (2002) Unravelling the composition of very complex samples by comprehensive gas chromatography coupled to time-of-flight mass spectrometry: Cigarette smoke. *J Chromatogr A* 974: 169-184
4. Takanami Y, Chida M, Hasebe H, et al. (2003) Analysis of Cigarette Smoke by an Online Thermal Desorption System and Multidimensional GC-MS. *J Chromatogr Sci* 41: 317-322
5. Borgerding M, Klus H (2005) Analysis of complex mixtures -- Cigarette smoke. *Exp Toxicol Pathol* 57 Suppl 1: 43-73
6. Charles SM, Batterman SA, Jia C (2007) Composition and emissions of VOCs in main- and side-stream smoke of research cigarettes. *Atmos Environ* 41: 5371-5384
7. Adam T, Mitschke S, Baker RR (2009) Investigation of tobacco pyrolysis gases and puff-by-puff resolved cigarette smoke by single photon ionisation (SPI)-time-of-flight mass spectrometry (TOFMS). *Beitr Zur Tab Tob Res* 23: 203-226

8. Wang J, Weng J-J, Jia L-Y, et al. (2012) Study on Gas Phase Components in Mainstream Cigarette Smoke by Synchrotron Radiation Photoionization Mass Spectrometry. *Chin J Anal Chem* 40: 1048-1052
9. Counts ME, Hsu FS, Laffoon SW, et al. (2004) Mainstream smoke constituent yields and predicting relationships from a worldwide market sample of cigarette brands: ISO smoking conditions. *Regul Toxicol Pharmacol* 39: 111-134
10. Counts ME, Morton MJ, Laffoon SW, et al. (2005) Smoke composition and predicting relationships for international commercial cigarettes smoked with three machine-smoking conditions. *Regul Toxicol Pharmacol* 41: 185-227
11. Castro D, Slezakova K, Delerue-Matos C, et al. (2011) Polycyclic aromatic hydrocarbons in gas and particulate phases of indoor environments influenced by tobacco smoke: Levels, phase distributions, and health risks. *Atmos Environ* 45: 1799-1808
12. Li M, Dong J-G, Huang Z-X, et al. (2012) Analysis of Cigarette Smoke Aerosol by Single Particle Aerosol Mass Spectrometer. *Chin J Anal Chem* 40: 936-939
13. Wright C (2015) Standardized methods for the regulation of cigarette-smoke constituents. *Trends Anal Chem* 66: 118-127
14. Ding YS, Zhang L, Jain RB, et al. (2008) Levels of Tobacco-Specific Nitrosamines and Polycyclic Aromatic Hydrocarbons in Mainstream Smoke from Different Tobacco Varieties. *Cancer Epidemiol Biomarkers Prev* 17: 3366-3371
15. Ding YS, Trommel JS, Yan XJ, et al. (2005) Determination of 14 Polycyclic Aromatic Hydrocarbons in Mainstream Smoke from Domestic Cigarettes. *Environ Sci Technol* 39: 471-478
16. Lu X, Cai J, Kong H, et al. (2003) Analysis of Cigarette Smoke Condensates by Comprehensive Two-Dimensional Gas Chromatography/Time-of-Flight Mass Spectrometry I Acidic Fraction. *Anal Chem* 75: 4441-4451
17. Lu X, Zhao M, Kong H, et al. (2004) Characterization of cigarette smoke condensates by comprehensive two-dimensional gas chromatography/time-of-flight mass spectrometry (GC×GC/TOFMS) Part 2: Basic fraction. *J Sep Sci* 27: 101-109
18. Brokl M, Bishop L, Wright CG, et al. (2013) Analysis of mainstream tobacco smoke particulate phase using comprehensive two-dimensional gas chromatography time-of-flight mass spectrometry. *J Sep Sci* 36: 1037-1044
19. Hughey CA, Rodgers RP, Marshall AG (2002) Resolution of 11 000 Compositionally Distinct Components in a Single Electrospray Ionization Fourier Transform Ion Cyclotron Resonance Mass Spectrum of Crude Oil. *Anal Chem* 74: 4145-4149
20. Rodgers RP, Schaub TM, Marshall AG (2005) Petroleomics: MS Returns to Its Roots. *Anal Chem* 77: 20-A
21. Hertkorn N, Ruecker C, Meringer M, et al. (2007) High-precision frequency measurements: indispensable tools at the core of the molecular-level analysis of complex systems. *Anal Bioanal Chem* 389: 1311-1327
22. Kujawinski EB (2002) Electrospray Ionization Fourier Transform Ion Cyclotron Resonance Mass Spectrometry (ESI FT-ICR MS): Characterization of Complex Environmental Mixtures. *Environ Forensics* 3: 207-216

23. Schmitt-Kopplin P, Gelencsér A, Dabek-Zlotorzynska E, et al. (2010) Analysis of the Unresolved Organic Fraction in Atmospheric Aerosols with Ultrahigh-Resolution Mass Spectrometry and Nuclear Magnetic Resonance Spectroscopy: Organosulfates As Photochemical Smog Constituents. *Anal Chem* 82: 8017-8026
24. Gonsior M, Zwartjes M, Cooper WJ, et al. (2011) Molecular characterization of effluent organic matter identified by ultrahigh resolution mass spectrometry. *Water Res* 45: 2943-2953
25. Cottrell BA, Gonsior M, Isabelle LM, et al. (2013) A regional study of the seasonal variation in the molecular composition of rainwater. *Atmos Environ* 77: 588-597
26. Cortés-Francisco N, Harir M, Lucio M, et al. (2014) High-field FT-ICR mass spectrometry and NMR spectroscopy to characterize DOM removal through a nanofiltration pilot plant. *Water Res* 67: 154-165
27. Gonsior M, Schmitt-Kopplin P, Stavklint H, et al. (2014) Changes in Dissolved Organic Matter during the Treatment Processes of a Drinking Water Plant in Sweden and Formation of Previously Unknown Disinfection Byproducts. *Environ Sci Technol* 48: 12714-12722
28. Schramm S, Carré V, Scheffler J-L, et al. (2011) Analysis of Mainstream and Sidestream Cigarette Smoke Particulate Matter by Laser Desorption Mass Spectrometry. *Anal Chem* 83: 133-142
29. Schramm S, Carré V, Scheffler J-L, et al. (2014) Active and passive smoking - New insights on the molecular composition of different cigarette smoke aerosols by LDI-FTICRMS. *Atmos Environ* 92: 411-420
30. Schäfer M, Drayß M, Springer A, et al. (2007) Radical Cations in Electrospray Mass Spectrometry: Formation of Open-Shell Species, Examination of the Fragmentation Behaviour in ESI-MSn and Reaction Mechanism Studies by Detection of Transient Radical Cations. *Eur J Org Chem* 2007: 5162-5174
31. Cole DP, Smith EA, Dalluge D, et al. (2013) Molecular characterization of nitrogen-containing species in switchgrass bio-oils at various harvest times. *Fuel* 111: 718-726
32. Sudasinghe N, Dungan B, Lammers P, et al. (2014) High resolution FT-ICR mass spectral analysis of bio-oil and residual water soluble organics produced by hydrothermal liquefaction of the marine microalga Nannochloropsis salina. *Fuel* 119: 47-56
33. Baker RR (1987) A review of pyrolysis studies to unravel reaction steps in burning tobacco. *J Anal Appl Pyrolysis* 11: 555-573
34. Wu Z, Rodgers RP, Marshall AG (2004) Two- and Three-Dimensional van Krevelen Diagrams: A Graphical Analysis Complementary to the Kendrick Mass Plot for Sorting Elemental Compositions of Complex Organic Mixtures Based on Ultrahigh-Resolution Broadband Fourier Transform Ion Cyclotron Resonance Mass Measurements. *Anal Chem* 76: 2511-2516
35. Cho Y, Ahmed A, Islam A, et al. (2015) Developments in FT-ICR MS instrumentation, ionization techniques, and data interpretation methods for petroleomics. *Mass Spectrom Rev* 34: 248-263
36. Baker RR, Bishop LJ (2004) The pyrolysis of tobacco ingredients. *J Anal Appl Pyrolysis* 71: 223-311
37. Mullen CA, Boateng AA (2008) Chemical Composition of Bio-oils Produced by Fast Pyrolysis of Two Energy Crops †. *Energy Fuels* 22: 2104-2109
38. Olcese R, Carré V, Aubriet F, et al. (2013) Selectivity of Bio-oils Catalytic Hydrotreatment Assessed by Petroleomic and GC*GC/MS-FID Analysis. *Energy Fuels* 27: 2135-2145

39. Li S, Olegario RM, Banyasz JL, et al. (2003) Gas chromatography-mass spectrometry analysis of polycyclic aromatic hydrocarbons in single puff of cigarette smoke. *J Anal Appl Pyrolysis* 66: 155-163
40. Carré V, Aubriet F, Muller J-F (2005) Analysis of cigarette smoke by laser desorption mass spectrometry. *Anal Chim Acta* 540: 257-268
41. Aubriet F, Carré V (2010) Potential of laser mass spectrometry for the analysis of environmental dust particles—A review. *Anal Chim Acta* 659: 34-54
42. Cho Y, Witt M, Kim YH, et al. (2012) Characterization of Crude Oils at the Molecular Level by Use of Laser Desorption Ionization Fourier-Transform Ion Cyclotron Resonance Mass Spectrometry. *Anal Chem* 84: 8587-8594
43. Cho Y, Jin JM, Witt M, et al. (2013) Comparing Laser Desorption Ionization and Atmospheric Pressure Photoionization Coupled to Fourier Transform Ion Cyclotron Resonance Mass Spectrometry To Characterize Shale Oils at the Molecular Level. *Energy Fuels* 27: 1830-1837
44. Le Brech Y, Delmotte L, Raya J, et al. (2015) High Resolution Solid State 2D NMR Analysis of Biomass and Biochar. *Anal Chem* 87: 843-847

AIMS Press